Gates, States, and Circuits:

Notes on the circuit model of quantum computation

Tech. Note 014v3 http://threeplusone.com/gates

Gavin E. Crooks

2020-02-13

Contents

1 Single qubit gates

1.1 Pauli gates

The simplest 1-qubit gates are the 4 gates represented by the Pauli operators: I, X, Y, and Z.

Pauli-I (identity):

$$\begin{pmatrix} 1 & 0 \\ 0 & 1 \end{pmatrix}$$

The trivial no-operation gate on 1-qubit, represented by the identity matrix.

Pauli-X gate (X-gate, NOT, bit flip)

$$\begin{pmatrix} 0 & 1 \\ 1 & 0 \end{pmatrix}$$

Applies a logical not to the computational basis, so that $|0\rangle$ becomes $|1\rangle$ and $|1\rangle$ becomes $|0\rangle$.

Pauli-Y gate (Y-gate) :

$$\begin{pmatrix} 0 & -i \\ i & 0 \end{pmatrix}$$

A useful mnemonic for remembering the matrix of the Y gate is "Minus eye high" [**?**].

Classically, there are only 2 1-bit logic gates, identity and NOT. But in quantum mechanics the zero and one states can be placed into superposition, so there are many other possibilities.

Pauli-Z gate (Z-gate, phase flip)

$$\begin{pmatrix} 1 & 0 \\ 0 & -1 \end{pmatrix}$$

Phase gate

1.2 Rotation gates

R_x gate

R_z gate

R_y gate

1.3 Powers of Pauli gates

Phase shift gate

S (Phase, P, 'ess') gate

$$\begin{pmatrix} 1 & 0 \\ 0 & i \end{pmatrix}$$

T ("tee", $\pi/8$) gate

$$\begin{pmatrix} 1 & 0 \\ 0 & e^{i\pi/4} \end{pmatrix}$$

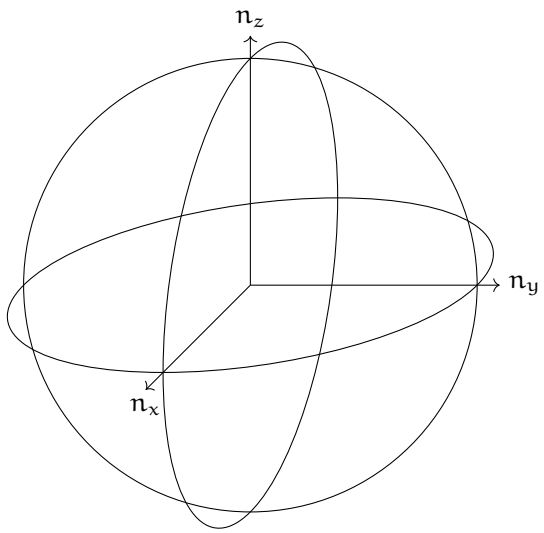

Figure 1: Sphere of 1-qubit gates. Each point within this sphere represents a unique (up to phase) 1-qubit gate. Antipodal points on the surface represent the same gate.

1.4 Hadamard-type gates

Hadamard gate

$$\begin{bmatrix} 1 & 1 \\ 1 & -1 \end{bmatrix}$$

Pseudo-Hadamard gate [**?**]

$$\frac{1}{\sqrt{2}}\begin{bmatrix} 1 & 1 \\ -1 & 1 \end{bmatrix}$$

$$\frac{1}{\sqrt{2}}\begin{bmatrix} 1 & -1 \\ 1 & 1 \end{bmatrix}$$

$R_x(\theta)$

$R_y(\theta)$

$R_z(\theta)$

$R_{\vec{n}}(\theta)$

$$R_{\vec{n}}(\theta) = \cos\frac{\theta}{2}I - i\sin\frac{\theta}{2}(n_x X + n_y Y + n_z Z) \qquad (1)$$

2 Decomposition of 1-qubit gates

2.1 ZYZ-Euler decompositions

2.2 General Euler decompositions

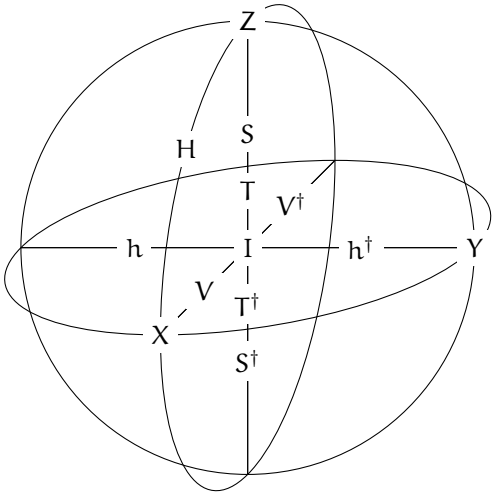

Figure 2: Coordinates of common 1-qubit gates

2.3 Bloch rotation decomposition

3 The canonical gate

The canonical gate is a 3-parameter quantum logic gate that acts on two qubits [**? ? ?**].

$$\begin{aligned}&\mathrm{CAN}(t_x, t_y, t_z)\\ &\quad= \exp\Big(-i\frac{\pi}{2}(t_x X\otimes X + t_y Y\otimes Y + t_z Z\otimes Z)\Big)\end{aligned} \tag{2}$$

Here, $X = \left(\begin{smallmatrix}0 & 1\\ 1 & 0\end{smallmatrix}\right)$, $Y = \left(\begin{smallmatrix}0 & -i\\ i & 0\end{smallmatrix}\right)$, and $Z = \left(\begin{smallmatrix}1 & 0\\ 0 & -1\end{smallmatrix}\right)$ are the 1-qubit Pauli matrices.

Note that other parameterizations are common in the literature. Often there will be a sign flip and/or the $\frac{\pi}{2}$ factor is absorbed into the parameters. The parameterization used here the nice feature that it corresponds to powers of direct products of Pauli operators (up to phase) (see (8), (12), (**??**)) .

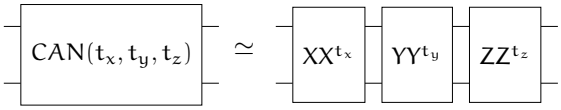

The canonical gate is, in a sense, the elementary 2-qubit gate, since any other 2-qubit gate can be decomposed into a canonical gate, and local 1-qubit interactions [1, 2, 3, 4].

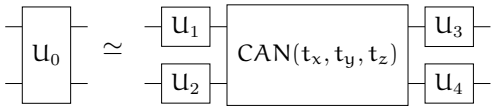

Here we use '$\simeq$' to indicate that two gates have the same unitary operator up to a global (and generally irrelevant) phase factor. We'll use '$\sim$' to indicate that two gates are locally equivalent, in that they can be mapped to one another by local 1-qubit rotations.

The canonical gate is periodic in each parameters with period 4, or period 2 if we neglect a -1 global phase factor. Thus we can constrain each parameter to the range $[-1, 1)$. Since $X\otimes X$, $Y\otimes Y$, and $Z\otimes Z$ all commute, the parameter space has the topology of a 3-torus.

However, the canonical coordinates of any given 2-qubit gate are not unique since we have considerable freedom in the prepended and apended local gates. To remove these symmetries we can constraint the canonical parameters to a "Weyl chamber" [**? ?**].

$$(\tfrac{1}{2} \geqslant t_x \geqslant t_y \geqslant t_z \geqslant 0) \cup (\tfrac{1}{2} \geqslant (1-t_x) \geqslant t_y \geqslant t_z > 0) \tag{3}$$

This Weyl chamber forms a trirectangular tetrahedron. All gates in the Weyl chamber are locally inequivalent (They cannot be obtained from each other via local 1-qubit gates). The net of the Weyl chamber is illustrated in Fig. 3, and the coordinates of many common 2-qubit gates are listed in table 1. Code for performing a canonical-decomposition, and therefore of determining the Weyl coordinates, can be found in the decompositions subpackage of `QuantumFlow` [5].

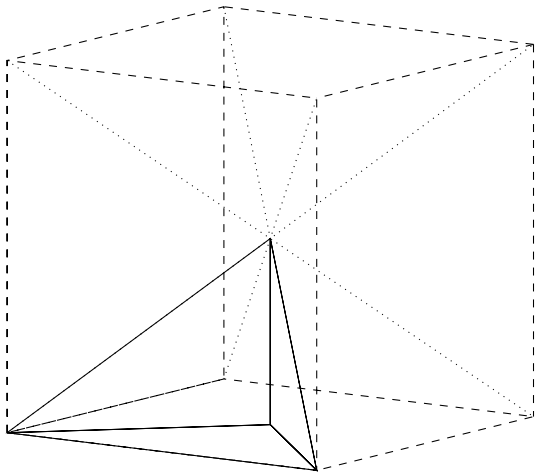

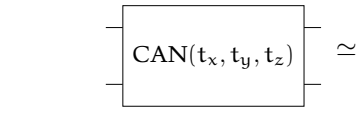

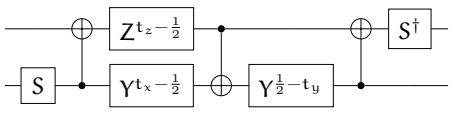

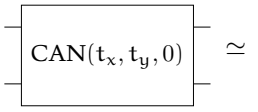

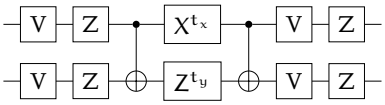

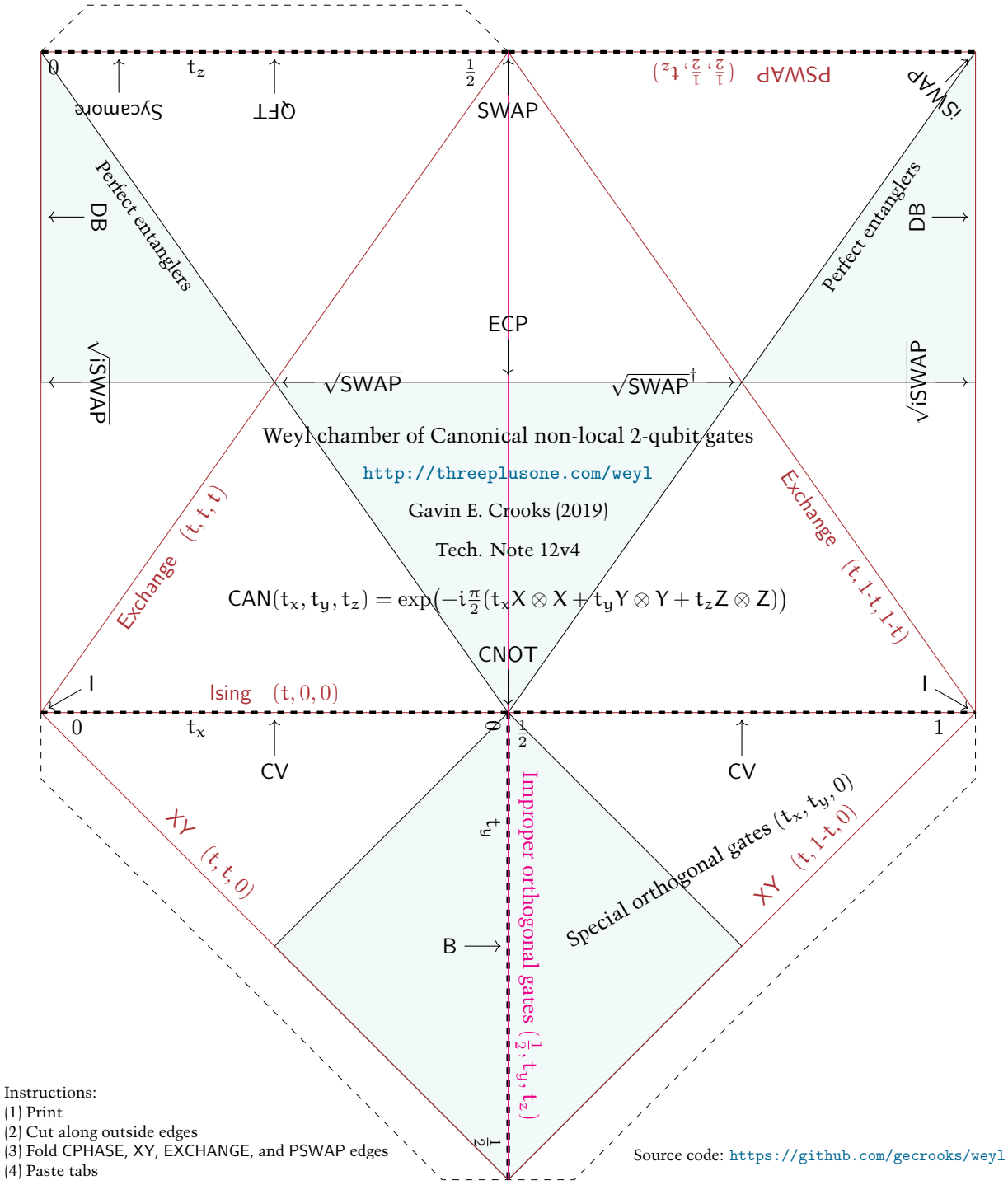

Instructions:
(1) Print
(2) Cut along outside edges
(3) Fold CPHASE, XY, EXCHANGE, and PSWAP edges
(4) Paste tabs

Source code: https://github.com/gecrooks/weyl

Figure 3: The Weyl chamber of canonical non-local 2 qubit gates. (Print, cut, fold, and paste)

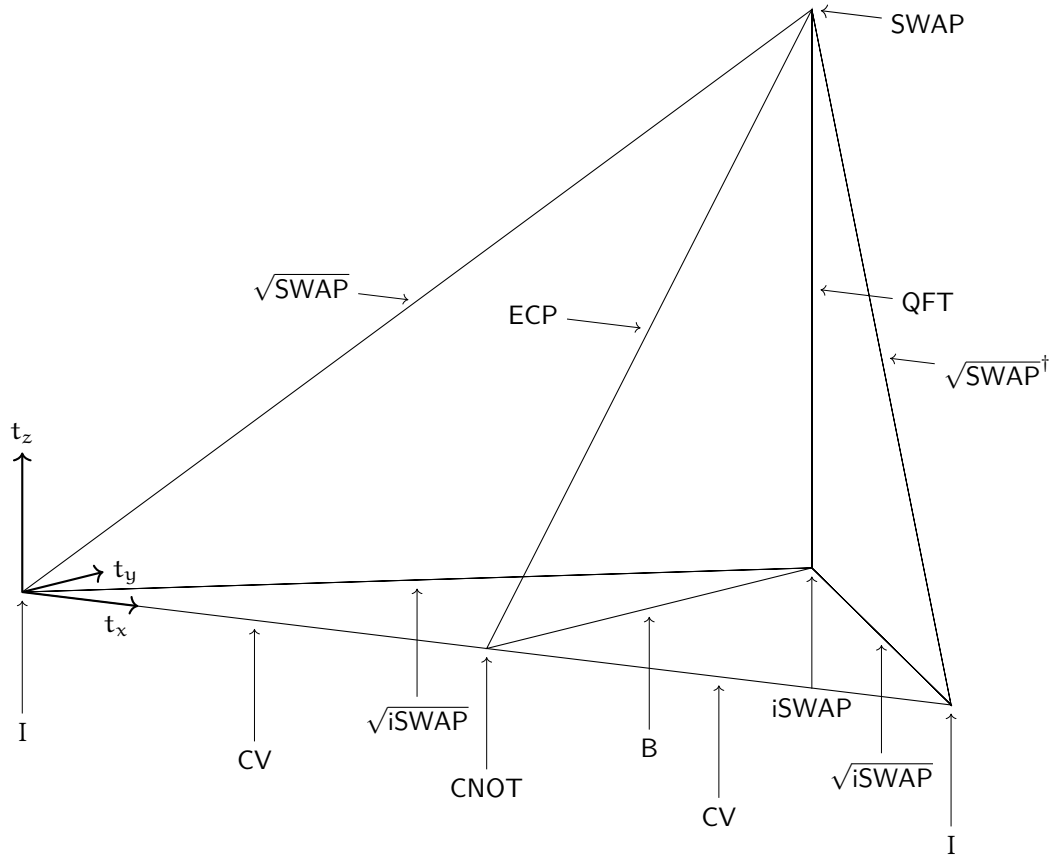

Figure 4: Location of the 11 principal 2-qubit gates in the Weyl chamber. All of these gates have coordinates of the form $\mathsf{CAN}(\frac{1}{4}\mathrm{k_x}, \frac{1}{4}\mathrm{k_y}, \frac{1}{4}\mathrm{k_z})$, for integer $\mathrm{k_x}$, $\mathrm{k_y}$, and $\mathrm{k_z}$. Note there is a symmetry on the bottom face such that $\mathsf{CAN}(\mathrm{t_x}, \mathrm{t_y}, 0) \sim \mathsf{CAN}(\frac{1}{2} - \mathrm{t_x}, \mathrm{t_y}, 0)$.

Table 1: Canonical coordinates of common 2-qubit gates

Gate	t_x	t_y	t_z	t'_x	t'_y	t'_z
	$\leqslant\frac{1}{2}$			$>\frac{1}{2}$		
I_2	0	0	0	1	0	0
CNOT / CZ / MS	$\frac{1}{2}$	0	0			
iSWAP / DCNOT	$\frac{1}{2}$	$\frac{1}{2}$	0	$\frac{3}{4}$	$\frac{1}{2}$	0
SWAP	$\frac{1}{2}$	$\frac{1}{2}$	$\frac{1}{2}$			
CV	$\frac{1}{4}$	0	0	$\frac{3}{4}$	0	0
$\sqrt{\text{iSWAP}}$	$\frac{1}{4}$	$\frac{1}{4}$	0	$\frac{3}{4}$	$\frac{1}{4}$	0
DB	$\frac{3}{8}$	$\frac{3}{8}$	0	$\frac{5}{8}$	$\frac{3}{8}$	0
$\sqrt{\text{SWAP}}$	$\frac{1}{4}$	$\frac{1}{4}$	$\frac{1}{4}$			
$\sqrt{\text{SWAP}}^\dagger$				$\frac{3}{4}$	$\frac{1}{4}$	$\frac{1}{4}$
B	$\frac{1}{2}$	$\frac{1}{4}$	0			
ECP	$\frac{1}{2}$	$\frac{1}{4}$	$\frac{1}{4}$			
QFT_2	$\frac{1}{2}$	$\frac{1}{2}$	$\frac{1}{4}$			
Sycamore	$\frac{1}{2}$	$\frac{1}{2}$	$\frac{1}{12}$			
Ising / CPHASE	t	0	0			
XY	t	t	0	t	1-t	0
Exchange / SWAP^α	t	t	t	t	1-t	1-t
PSWAP	$\frac{1}{2}$	$\frac{1}{2}$	t			
Special orthogonal	t_x	t_y	0			
Improper orthogonal	$\frac{1}{2}$	t_y	t_z			
XXY	t	t	δ	t	1-t	δ
	δ	t	t	δ	t	t

4 Principal 2-qubit gates

4.1 Clifford gates

There are four unique 2-qubits gates in the Clifford group (up to local 1-qubit Cliffords): the identity, CNOT, iSWAP, and SWAP gates.

Identity gate

$$I_2 = \begin{pmatrix} 1&0&0&0\\ 0&1&0&0\\ 0&0&1&0\\ 0&0&0&1 \end{pmatrix} = \text{CAN}(0,0,0) \tag{4}$$

Controlled-NOT gate (CNOT, controlled-X, CX)

$$\text{CNOT} = \begin{pmatrix} 1&0&0&0\\ 0&1&0&0\\ 0&0&0&1\\ 0&0&1&0 \end{pmatrix} \sim \text{CAN}(\tfrac{1}{2},0,0) \tag{5}$$

Commonly represented by the circuit diagrams

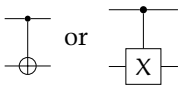

The CNOT gate is not symmetric between the two qubits. But we can switch control • and target ⊕ with local Hadamard gates.

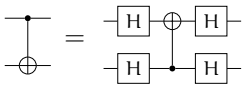

iSWAP-gate

$$\text{iSWAP} = \begin{pmatrix} 1&0&0&0\\ 0&0&i&0\\ 0&i&0&0\\ 0&0&0&1 \end{pmatrix} \simeq \text{CAN}(-\tfrac{1}{2},-\tfrac{1}{2},0) \tag{6}$$

SWAP-gate

$$\text{SWAP} = \begin{pmatrix} 1&0&0&0\\ 0&0&1&0\\ 0&1&0&0\\ 0&0&0&1 \end{pmatrix} \simeq \text{CAN}(\tfrac{1}{2},\tfrac{1}{2},\tfrac{1}{2}) \tag{7}$$

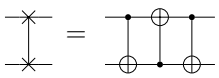

4.2 XX gates

Gates in the XX (or Ising) class have coordinates $\text{CAN}(t,0,0)$, which forms the front edge of the Weyl chamber. This includes the identity and CNOT gates.

XX gate (Ising)

$$\begin{aligned}\mathrm{XX}(t) &= e^{-i\frac{\pi}{2}t\,X\otimes X} \\ &= \begin{pmatrix} \cos(\frac{\pi}{2}t) & 0 & 0 & -i\sin(\frac{\pi}{2}t) \\ 0 & \cos(\frac{\pi}{2}t) & -i\sin(\frac{\pi}{2}t) & 0 \\ 0 & -i\sin(\frac{\pi}{2}t) & \cos(\frac{\pi}{2}t) & 0 \\ -i\sin(\frac{\pi}{2}t) & 0 & 0 & \cos(\frac{\pi}{2}t) \end{pmatrix} \\ &= \mathrm{CAN}(t,0,0)\end{aligned} \tag{8}$$

Mølmer-Sørensen gate (MS) [? ?]

$$\begin{aligned}\mathrm{MS} &= \frac{1}{\sqrt{2}}\begin{pmatrix} 1 & 0 & 0 & i \\ 0 & 1 & i & 0 \\ 0 & i & 1 & 0 \\ i & 0 & 0 & 1 \end{pmatrix} \\ &= \mathrm{CAN}(-\tfrac{1}{2},0,0) \\ &\sim \mathrm{CAN}(\tfrac{1}{2},0,0) \\ &\sim \mathrm{CNOT}\end{aligned} \tag{9}$$

Proposed as a natural gate for laser driven trapped ions. Locally equivalent to CNOT. The Mølmer-Sørensen gate, or more exactly its complex conjugate $\mathrm{MS}^\dagger = \mathrm{CAN}(\frac{1}{2},0,0)$ is the natural canonical representation of the CNOT/CZ/MS gate family.

Magic gate (M) [? ? ?]

$$\mathrm{M} = \frac{1}{\sqrt{2}}\begin{bmatrix} 1 & i & 0 & 0 \\ 0 & 0 & i & 1 \\ 0 & 0 & i & -1 \\ 1 & -i & 0 & 0 \end{bmatrix} \tag{10}$$

$$\sim \mathrm{CAN}(\tfrac{1}{2},0,0) \tag{11}$$

[6]

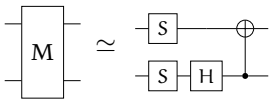

YY gate

$$\begin{aligned}\mathrm{YY}(t) &= e^{-i\frac{\pi}{2}t\,Y\otimes Y} \\ &= \begin{pmatrix} \cos(\frac{\pi}{2}t) & 0 & 0 & +i\sin(\frac{\pi}{2}t) \\ 0 & \cos(\frac{\pi}{2}t) & -i\sin(\frac{\pi}{2}t) & 0 \\ 0 & -i\sin(\frac{\pi}{2}t) & \cos(\frac{\pi}{2}t) & 0 \\ +i\sin(\frac{\pi}{2}t) & 0 & 0 & \cos(\frac{\pi}{2}t) \end{pmatrix} \\ &= \mathrm{CAN}(0,t,0) \\ &\sim \mathrm{CAN}(t,0,0)\end{aligned} \tag{12}$$

ZZ gate

$$\begin{aligned}\mathrm{ZZ}(t) &= e^{-i\frac{\pi}{2}t\,Z\otimes Z} \\ &= \begin{pmatrix} 1 & 0 & 0 & 0 \\ 0 & e^{-i\pi t} & 0 & 0 \\ 0 & 0 & e^{-i\pi t} & 0 \\ 0 & 0 & 0 & 1 \end{pmatrix} \\ &= \mathrm{CAN}(0,0,t) \\ &\sim \mathrm{CAN}(t,0,0)\end{aligned} \tag{13}$$

Controlled-Y gate

$$\begin{aligned}\mathrm{CY} &= \begin{pmatrix} 1 & 0 & 0 & 0 \\ 0 & 1 & 0 & 0 \\ 0 & 0 & 0 & -i \\ 0 & 0 & +i & 0 \end{pmatrix} \\ &\sim \mathrm{CAN}(\tfrac{1}{2},0,0)\end{aligned} \tag{14}$$

Commonly represented by the circuit diagram:

Controlled-Z gate (CZ or CSIGN)

$$\begin{aligned}\mathrm{CZ} &= \begin{pmatrix} 1 & 0 & 0 & 0 \\ 0 & 1 & 0 & 0 \\ 0 & 0 & 1 & 0 \\ 0 & 0 & 0 & -1 \end{pmatrix} \\ &\sim \mathrm{CAN}(\tfrac{1}{2},0,0)\end{aligned} \tag{15}$$

Commonly represented by the circuit diagrams

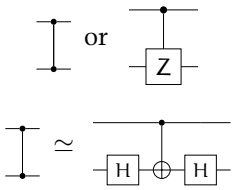

Controlled-V gate (square root of CNOT gate):

$$\begin{aligned}\mathrm{CV} &= \begin{pmatrix} 1 & 0 & 0 & 0 \\ 0 & 1 & 0 & 0 \\ 0 & 0 & \frac{1+i}{2} & \frac{1-i}{2} \\ 0 & 0 & \frac{1-i}{2} & \frac{1+i}{2} \end{pmatrix} \\ &\sim \mathrm{CAN}(\tfrac{1}{4},0,0)\end{aligned} \tag{16}$$

The CV gate is a square-root of CNOT, since the V-gate is the square root of the X-gate

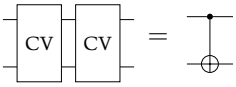

Note that the inverse $CV^\dagger$ is a distinct square-root of CNOT. However CV and $CV^\dagger$ are locally equivalent, which is a consequence of the symmetry about $t_x = \frac{1}{2}$ on the bottom face of the Weyl chamber.

4.3 XY gates

Gates in the XY class forms two edges of the Weyl chamber with coordinates $\mathrm{CAN}(t, t, 0)$ (for $t \leqslant \frac{1}{2}$) and $\mathrm{CAN}(t, 1-t, 0)$ (for $t > \frac{1}{2}$). This includes the identity and iSWAP gates.

XY-gate Also occasionally referred to as the piSWAP (or parametric iSWAP) gate.

$$\begin{aligned}\mathrm{XY}(t) &= \begin{pmatrix} 1 & 0 & 0 & 0 \\ 0 & \cos(\pi t) & -i\sin(\pi t) & 0 \\ 0 & -i\sin(\pi t) & \cos(\pi t) & 0 \\ 0 & 0 & 0 & 1 \end{pmatrix} \\ &= \mathrm{CAN}(t, t, 0) \\ &\sim \mathrm{CAN}(t, 1-t, 0)\end{aligned} \tag{17}$$

Double Controlled NOT gate (DCNOT)

$$\begin{aligned}\mathrm{DCNOT} &= \begin{bmatrix} 1 & 0 & 0 & 0 \\ 0 & 0 & 0 & 1 \\ 0 & 1 & 0 & 0 \\ 0 & 0 & 1 & 0 \end{bmatrix} \\ &\sim \mathrm{CAN}(\tfrac{1}{2}, \tfrac{1}{2}, 0)\end{aligned} \tag{18}$$

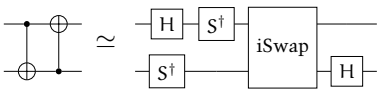

Givens gate

$$\mathrm{Givens} = \exp(-i\theta(Y \otimes X - X \otimes Y)/2) \tag{19}$$

$$= \begin{bmatrix} 1 & 0 & 0 & 0 \\ 0 & \cos(\theta) & -\sin(\theta) & 0 \\ 0 & \sin(\theta) & \cos(\theta) & 0 \\ 0 & 0 & 0 & 1 \end{bmatrix} \tag{20}$$

$$\sim \mathrm{CAN}(\tfrac{1}{2}, \tfrac{1}{2}, 0)$$

bSWAP (Bell-Rabi) gate [?]

$$\begin{aligned}\mathrm{bSWAP} &= \begin{pmatrix} 0 & 0 & 0 & -i \\ 0 & 1 & 0 & 0 \\ 0 & 0 & 1 & 0 \\ -i & 0 & 0 & 0 \end{pmatrix} \\ &= \mathrm{CAN}(\tfrac{1}{2}, -\tfrac{1}{2}, 0) \\ &\sim \mathrm{CAN}(\tfrac{1}{2}, \tfrac{1}{2}, 0)\end{aligned} \tag{21}$$

???? gate

$$\begin{bmatrix} +1 & 0 & 0 & 0 \\ 0 & +1 & +1 & 0 \\ 0 & -1 & +1 & 0 \\ 0 & 0 & 0 & +1 \end{bmatrix} \tag{22}$$

$$\sim \mathrm{Can}(\tfrac{1}{2}, \tfrac{1}{2}, 0)$$

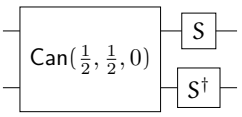

Dagwood Bumstead (DB) gate [7] Of all the gates in the XY class, the Dagwood Bumstead-gate makes the biggest sandwiches. [7, Fig. 4]

$$\begin{aligned}\mathrm{DB} &= \begin{pmatrix} 1 & 0 & 0 & 0 \\ 0 & \cos(\frac{3\pi}{8}) & -i\sin(\frac{3\pi}{8}) & 0 \\ 0 & -\sin(\frac{3\pi}{8}) & \cos(\frac{3\pi}{8}) & 0 \\ 0 & 0 & 0 & 1 \end{pmatrix} \\ &= \mathrm{XY}(\tfrac{3}{8}) \\ &= \mathrm{CAN}(\tfrac{3}{8}, \tfrac{3}{8}, 0)\end{aligned} \tag{23}$$

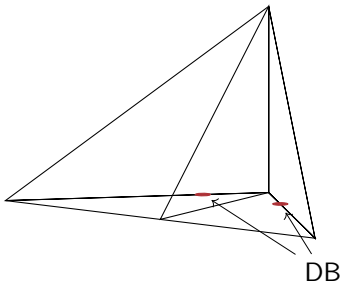

4.4 Exchange-interaction gates

Includes the identity and SWAP gates.

EXCH (XXX) gate

$$\mathrm{EXCH}(t) = \mathrm{CAN}(t, t, t) \tag{24}$$

SWAP-alpha gates

$$\mathrm{SWAP}^\alpha \sim \mathrm{CAN}(\alpha, \alpha, \alpha) \tag{25}$$

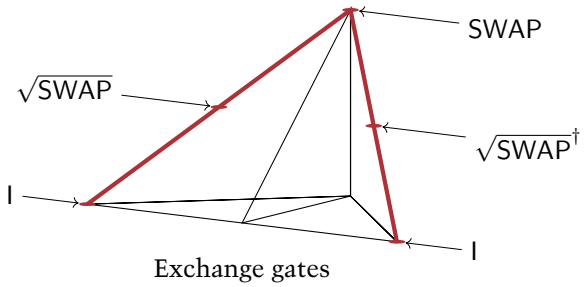

Exchange gates

$\sqrt{\mathrm{SWAP}}$-gate

$$\begin{aligned}\sqrt{\mathrm{SWAP}} &= \begin{pmatrix} 1 & 0 & 0 & 0 \\ 0 & \frac{1}{2}(1+i) & \frac{1}{2}(1-i) & 0 \\ 0 & \frac{1}{2}(1-i) & \frac{1}{2}(1+i) & 0 \\ 0 & 0 & 0 & 1 \end{pmatrix} \\ &= \mathrm{CAN}(\tfrac{1}{4}, \tfrac{1}{4}, \tfrac{1}{4})\end{aligned} \tag{26}$$

Inverse $\sqrt{\text{SWAP}}$-gate

$$\sqrt{\text{SWAP}}^\dagger = \begin{pmatrix} 1 & 0 & 0 & 0 \\ 0 & \frac{1}{2}(1-i) & \frac{1}{2}(1+i) & 0 \\ 0 & \frac{1}{2}(1+i) & \frac{1}{2}(1-i) & 0 \\ 0 & 0 & 0 & 1 \end{pmatrix} \tag{27}$$
$$= \text{CAN}(\tfrac{3}{4}, \tfrac{1}{4}, \tfrac{1}{4})$$

Because of the symmetry around $t_x = \frac{1}{2}$ on the base of the Weyl chamber, the CNOT and iSWAP gates only have one square root. But the SWAP has two locally distinct square roots, which are inverses of each other.

4.5 Parametric SWAP gates

The class of parametric SWAP (PSWAP) gates forms the back edge of the Weyl chamber, $\text{CAN}(\frac{1}{2}, \frac{1}{2}, t_z)$, connecting the SWAP and iSWAP gates. These gates can be decomposed into a SWAP and ZZ gate.

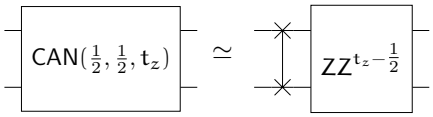

pSwap gate (parametric swap) [8] The parametric swap gate as originally defined in the QUIL quantum programming language.

$$\text{pSWAP}(\theta) = \begin{pmatrix} 1 & 0 & 0 & 0 \\ 0 & 0 & e^{i\theta} & 0 \\ 0 & e^{i\theta} & 0 & 0 \\ 0 & 0 & 0 & 1 \end{pmatrix} \tag{28}$$
$$\sim \text{CAN}(\tfrac{1}{2}, \tfrac{1}{2}, \tfrac{1}{2} - \tfrac{\theta}{\pi}) \tag{29}$$

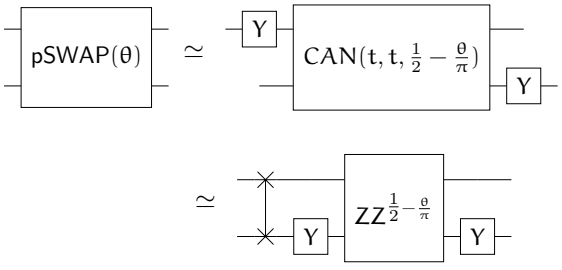

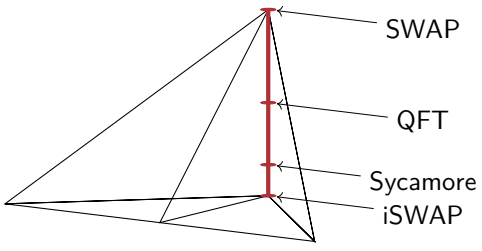

pSWAP gates

Quantum Fourier transform (QFT) [?]

$$\text{QFT} = \tfrac{1}{2}\begin{bmatrix} 1 & 1 & 1 & 1 \\ 1 & i & -1 & -i \\ 1 & -1 & 1 & -1 \\ 1 & -i & -1 & i \end{bmatrix} \tag{30}$$
$$\sim \text{CAN}(\tfrac{1}{2}, \tfrac{1}{2}, \tfrac{1}{4})$$

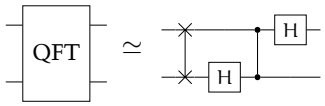

4.6 Orthogonal gates

An orthogonal gate, in this context, is a gate that can be represented by an orthogonal matrix (up to local 1-qubit rotations.) The special orthogonal gates have determinant $+1$ and coordinates $\text{CAN}(t_x, t_y, 0)$, which covers the bottom surface of the canonical Weyl chamber.

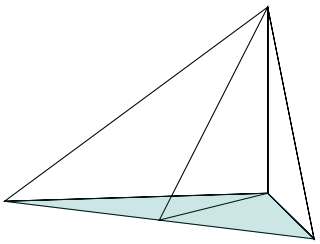

Special orthogonal gates

The improper orthogonal gates have determinant -1 and coordinates $\text{CAN}(\frac{1}{2}, t_y, t_z)$, which is a plane connecting the CNOT, iSWAP, and SWAP gates.

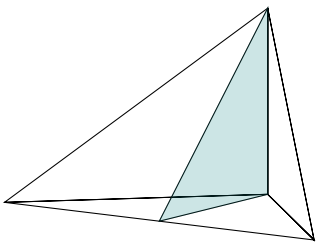

Improper orthogonal gates

B (Berkeley) gate [9] Located in the middle of the bottom face of the Weyl chamber.

$$\text{B} = \begin{pmatrix} \cos(\frac{\pi}{8}) & 0 & 0 & i\sin(\frac{\pi}{8}) \\ 0 & \cos(\frac{3\pi}{8}) & i\sin(\frac{3\pi}{8}) & 0 \\ 0 & i\sin(\frac{3\pi}{8}) & \cos(\frac{3\pi}{8}) & 0 \\ i\sin(\frac{\pi}{8}) & 0 & 0 & \cos(\frac{\pi}{8}) \end{pmatrix} \tag{31}$$
$$= \frac{\sqrt{2-\sqrt{2}}}{2}\begin{pmatrix} 1+\sqrt{2} & 0 & 0 & i \\ 0 & 1 & i(1+\sqrt{2}) & 0 \\ 0 & i(1+\sqrt{2}) & 1 & 0 \\ i & 0 & 0 & 1+\sqrt{2} \end{pmatrix}$$
$$= \text{CAN}(-\tfrac{1}{2}, -\tfrac{1}{4}, 0)$$

The B-gate, as originally defined, has canonical parameters outside our Weyl chamber due to differing conventions for parameterization of the canonical gate. But of

course it can be moved into our Weyl chamber with local gates.

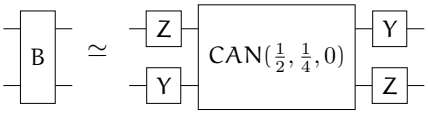

The B-gate is half way between the CNOT and DCNOT (~ iSWAP) gates, and thus it can be constructed from 3 CV (square root of CNOT) gates.

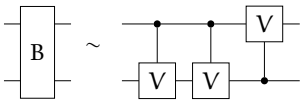

Notably two-B gates are sufficient to create any other 2-qubit gate (whereas, for example, we need 3 CNOT's in general) [9] [1]

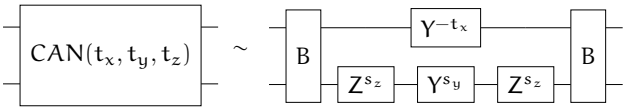

$$s_y = +\tfrac{1}{\pi}\arccos\left(1 - 4\sin^2\tfrac{1}{2}\pi t_y \cos^2\tfrac{1}{2}\pi t_z\right)$$
$$s_z = -\tfrac{1}{\pi}\arcsin\sqrt{\frac{\cos\pi t_y \cos\pi t_z}{1 - 2\sin^2\tfrac{1}{2}\pi t_y \cos^2\tfrac{1}{2}\pi t_z}} \qquad (32)$$

ECP-gate [7]

$$\mathsf{ECP} = \frac{1}{2}\begin{pmatrix} 2c & 0 & 0 & -i2s \\ 0 & (1+i)(c-s) & (1-i)(c+s) & 0 \\ 0 & (1-i)(c+s) & (1+i)(c-s) & 0 \\ -i2s & 0 & 0 & 2c \end{pmatrix} \qquad (33)$$
$$c = \cos(\tfrac{\pi}{8}) = \sqrt{\tfrac{2+\sqrt{2}}{2}}$$
$$s = \sin(\tfrac{\pi}{8}) = \sqrt{\tfrac{2-\sqrt{2}}{2}}$$
$$= \mathsf{CAN}(\tfrac{1}{2}, \tfrac{1}{4}, \tfrac{1}{4})$$

The peak of the pyramid of gates in the Weyl chamber that can be created with a square-root of iSWAP sandwich. Equivalent to $\mathsf{Can}(\frac{1}{2}, \frac{1}{4}, \frac{1}{4})$.

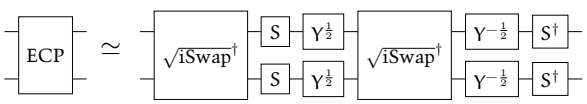

[1] Zang et al.[9] derive the analytic decomposition of the canonical gate to a B gate sandwich only up to local gates. Open Problem: Derive an analytic formula for the necessary local gates to complete the canonical to B-sandwich circuit above.

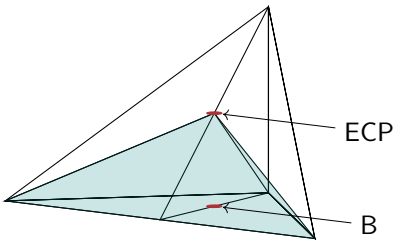

B and ECP gates, and ECP pyramid

W-gate [?]

$$\mathsf{W} = \begin{bmatrix} 1 & 0 & 0 & 0 \\ 0 & \frac{1}{\sqrt{2}} & \frac{1}{\sqrt{2}} & 0 \\ 0 & \frac{1}{\sqrt{2}} & -\frac{1}{\sqrt{2}} & 0 \\ 0 & 0 & 0 & 1 \end{bmatrix} \qquad (34)$$
$$\sim \mathsf{ECP} = \mathsf{CAN}(\tfrac{1}{2}, \tfrac{1}{4}, \tfrac{1}{4})$$

A 2-qubit orthogonal and Hermitian gate (and therefore also symmetric) $\mathsf{W}^\dagger = \mathsf{W}$, that applies a Hadamard gate to a duel-rail encoded qubit.

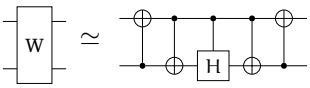

This W gate is locally equivalent to ECP,

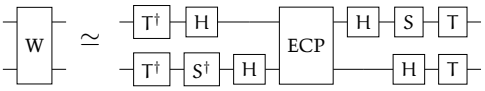

and thus three CNOT gates are necessary (and sufficient) to generate the gate.

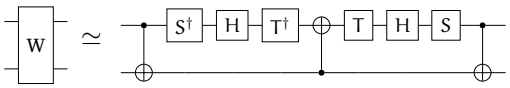

4.7 XXY gates

The remaining faces of the Weyl chamber are the XXY family. Thanks to the Weyl symmetries, this family covers all three faces that meet at the SWAP gate.

$$\mathsf{XXY}(t, \delta) = \mathsf{CAN}(t, t, \delta) \qquad (35)$$

FSIM (Ferminoic Simulator) gate [?]

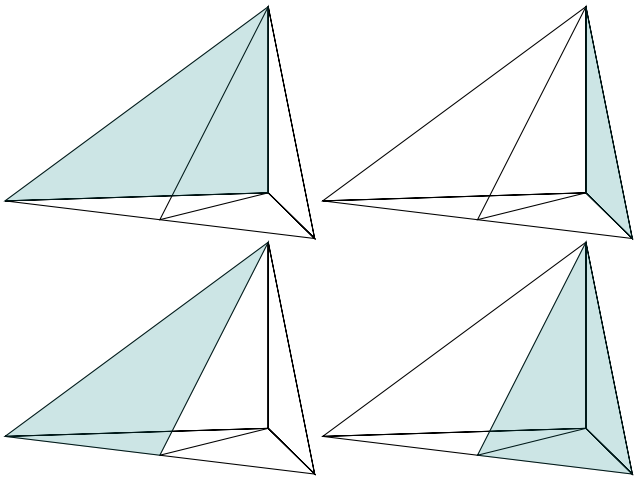

Sycamore **gate** [?]

4.8 Perfect entanglers

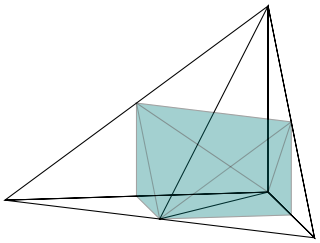

Perfect entaglers

5 Multi-qubit gates

Toffoli gate (controlled-controlled-not, CCNOT)

$$\begin{bmatrix} 1&0&0&0&0&0&0&0\\ 0&1&0&0&0&0&0&0\\ 0&0&1&0&0&0&0&0\\ 0&0&0&1&0&0&0&0\\ 0&0&0&0&1&0&0&0\\ 0&0&0&0&0&1&0&0\\ 0&0&0&0&0&0&0&1\\ 0&0&0&0&0&0&1&0 \end{bmatrix} \tag{36}$$

CCZ gate (controlled-controlled-Z)

$$\begin{bmatrix} 1&0&0&0&0&0&0&0\\ 0&1&0&0&0&0&0&0\\ 0&0&1&0&0&0&0&0\\ 0&0&0&1&0&0&0&0\\ 0&0&0&0&1&0&0&0\\ 0&0&0&0&0&1&0&0\\ 0&0&0&0&0&0&1&0\\ 0&0&0&0&0&0&0&-1 \end{bmatrix} \tag{37}$$

Fredkin gate (controlled-swap, CSWAP)

$$\begin{bmatrix} 1&0&0&0&0&0&0&0\\ 0&1&0&0&0&0&0&0\\ 0&0&1&0&0&0&0&0\\ 0&0&0&1&0&0&0&0\\ 0&0&0&0&1&0&0&0\\ 0&0&0&0&0&0&1&0\\ 0&0&0&0&0&1&0&0\\ 0&0&0&0&0&0&0&1 \end{bmatrix} \tag{38}$$

Deutsch gate [?] A controlled-controlled-$iR_x(2\theta)$ gate. Mostly of historical interest. This was the first quantum gate to be shown to be computationally universal.

$$\begin{bmatrix} 1&0&0&0&0&0&0&0\\ 0&1&0&0&0&0&0&0\\ 0&0&1&0&0&0&0&0\\ 0&0&0&1&0&0&0&0\\ 0&0&0&0&1&0&0&0\\ 0&0&0&0&0&1&0&0\\ 0&0&0&0&0&0&i\cos(\theta)&\sin(\theta)\\ 0&0&0&0&0&0&\sin(\theta)&i\cos(\theta) \end{bmatrix} \tag{39}$$

6 Controlled-Unitary gates

References

[1] Jun Zhang, Jiri Vala, Shankar Sastry, and K. Birgitta Whaley. Geometric theory of nonlocal two-qubit operations. *Phys. Rev. A*, 67:042313 (2003). doi:10.1103/PhysRevA.67.042313. arXiv:quant-ph/0209120. (page 3).

[2] Jun Zhang, Jiri Vala, Shankar Sastry, and K. Birgitta Whaley. Optimal quantum circuit synthesis from controlled-unitary gates. *Phys. Rev. A*, 69:042309 (2004). doi:10.1103/PhysRevA.69.042309. ArXiv:quant-ph/0308167. (page 3).

[3] M. Blaauboer and R. L. de Visser. An analytical decomposition protocol for optimal implementation of two-qubit entangling gates. *J. Phys. A : Math. Theor*, 41:395307 (2008). doi:10.1088/1751-8113/41/39/395307. arXiv:cond-mat/0609750. (page 3).

[4] Paul Watts, Maurice O'Connor, and Jir Vala. Metric structure of the space of two-qubit gates, perfect entanglers and quantum control. *Entropy*, 15:1963–1984 (2013). doi:10.3390/e15061963. (page 3).

[5] Gavin E. Crooks. QuantumFlow: A Quantum Algorithms Development Toolkit (2019). `https://quantumflow.readthedocs.io/`. (page 3).

[6] Farrokh Vatan and Colin Williams. Optimal quantum circuits for general two-qubit gates. *Phys. Rev. A*,

Table 2: Coordinates of the 24 1-qubit Clifford gates.

Gate	θ	n_x	n_y	n_z
I	0			
V	$\frac{1}{2}\pi$	1	0	0
X	π	1	0	0
$V^\dagger$	$-\frac{1}{2}\pi$	1	0	0
$h^\dagger$	$\frac{1}{2}\pi$	0	1	0
Y	π	0	1	0
h	$-\frac{1}{2}\pi$	0	1	0
S	$\frac{1}{2}\pi$	0	0	1
Z	π	0	0	1
$S^\dagger$	$-\frac{1}{2}\pi$	0	0	1
	π	$\frac{1}{\sqrt{2}}$	$\frac{1}{\sqrt{2}}$	0
	π	$\frac{1}{\sqrt{2}}$	0	$\frac{1}{\sqrt{2}}$
H	π	0	$\frac{1}{\sqrt{2}}$	$\frac{1}{\sqrt{2}}$
	π	$-\frac{1}{\sqrt{2}}$	$\frac{1}{\sqrt{2}}$	0
	π	$\frac{1}{\sqrt{2}}$	0	$-\frac{1}{\sqrt{2}}$
	π	0	$-\frac{1}{\sqrt{2}}$	$\frac{1}{\sqrt{2}}$
	$\frac{2}{3}\pi$	$\frac{1}{\sqrt{3}}$	$\frac{1}{\sqrt{3}}$	$\frac{1}{\sqrt{3}}$
	$-\frac{2}{3}\pi$	$\frac{1}{\sqrt{3}}$	$\frac{1}{\sqrt{3}}$	$\frac{1}{\sqrt{3}}$
	$\frac{2}{3}\pi$	$-\frac{1}{\sqrt{3}}$	$\frac{1}{\sqrt{3}}$	$\frac{1}{\sqrt{3}}$
	$-\frac{2}{3}\pi$	$-\frac{1}{\sqrt{3}}$	$\frac{1}{\sqrt{3}}$	$\frac{1}{\sqrt{3}}$
	$\frac{2}{3}\pi$	$\frac{1}{\sqrt{3}}$	$-\frac{1}{\sqrt{3}}$	$\frac{1}{\sqrt{3}}$
	$-\frac{2}{3}\pi$	$\frac{1}{\sqrt{3}}$	$-\frac{1}{\sqrt{3}}$	$\frac{1}{\sqrt{3}}$
	$\frac{2}{3}\pi$	$\frac{1}{\sqrt{3}}$	$\frac{1}{\sqrt{3}}$	$-\frac{1}{\sqrt{3}}$
	$-\frac{2}{3}\pi$	$\frac{1}{\sqrt{3}}$	$\frac{1}{\sqrt{3}}$	$-\frac{1}{\sqrt{3}}$

69:032315 (2004). doi:10.1103/PhysRevA.69.032315. ArXiv:quant-ph/0308006. (page 7).

[7] Eric C. Peterson, Gavin E. Crooks, and Robert S. Smith. Fixed-depth two-qubit circuits and the monodromy polytope. arXiv:1904.10541. (pages 8, 8, and 10).

[8] Robert S. Smith, Michael J. Curtis, and William J. Zeng. A practical quantum instruction set architecture. ArXiv:1608.03355. (page 9).

[9] Jun Zhang, Jiri Vala, Shankar Sastry, and K. Birgitta Whaley. Minimum construction of two-qubit quantum operations. *Phys. Rev. Lett.*, 93:020502 (2004). doi:10.1103/PhysRevLett.93.020502. Quant-ph/0312193. (pages 9, 10, and 10).

http://threeplusone.com/gates

typeset on 2020-02-13 with XeTeX version 0.99999
fonts: Trump Mediaeval (text), Euler (math)
2 7 1 8 2 8 1 8 3